EXAFS investigation of local structure of Er^{3+} and Yb^{3+} in low-silica calcium aluminate glasses

J. A. Sampaio* and S. Gama
Instituto de Física Gleb Wataghin, Universidade Estadual de Campinas, P.O. Box 6165, CEP 13083-970 Campinas SP, Brazil
(Received 4 July 2003; revised manuscript received 3 October 2003; published 17 March 2004)

Erbium and ytterbium environments in low-silica calcium aluminate glasses, with nominal composition 58 CaO, $27.1-x$ Al_2O_3, 6.9 MgO, 8 SiO_2, x Er_2O_3, or Yb_2O_3, $0.2 \leqslant x \leqslant 1.5$ (mol %), were investigated using x-ray-absorption fine-structure spectroscopy (EXAFS) on the Er and Yb L_{III} edge. The average Er-O bond separation was found to vary only slightly between 2.24 and 2.21 Å and the Yb-O bond between 2.20 and 2.18 Å. The first-shell coordination number decreased as the rare-earth oxide replaced Al_2O_3. For Er_2O_3-doped samples this decrease was about 28%, from 6.5 to 4.7 atoms, whereas for Yb_2O_3-doped ones it was about 14%, from 6.4 to 5.5 atoms. The decrease in the coordination number is attributed to the difficulty of rare-earth atoms to coordinate a larger number of the nonbridging oxygens that appear as the CaO/Al_2O_3 ratio decreases. The Debye-Waller factor $2\sigma^2$ varied from 0.026 to 0.012 $Å^2$.

DOI: 10.1103/PhysRevB.69.104203 PACS number(s): 61.10.Ht, 61.43.Fs

I. INTRODUCTION

Vacuum melted calcium aluminate (CA) glasses are transparent in the infrared spectral range up to 6 μm. Due to their highly refractory nature and excellent chemical durability, they are suitable for solid-state laser applications.[1] To achieve this aim, rare-earth (RE) atoms have to be introduced into the glass host, in order to obtain the spectroscopic properties of interest.[2] However, this RE addition in the glass composition promotes changes in the glass network, as well as in the envisaged spectroscopic properties, for example fluorescence quantum efficiency and lifetime of fluorescence.[3] Several quenching processes, such as energy transfer, cross-relaxation, and cooperative upconversion, are related to the interaction among the RE ions in the host.[3–5] In pure silica, only very small amounts of RE can be incorporated before microscopic clustering and ion-ion interactions appear.[3,5] In the case of phosphate glasses,[6] it is possible to introduce about 25 mol % of RE and only one-tenth of this amount in CA glasses.[7] In oxide glasses, the RE ions act as glass network modifiers because of their difficulty in taking lower coordination, which is attributed to the strong ionicity of the Ln-O bonds.[8] On the other hand, the RE ions are glass-forming in fluorozirconate glasses.[9] Considering these facts, the consequent changes of the RE environment have to be investigated.

Chemically specific structural properties, such as interatomic distances, coordination numbers, and degree of disorder in multicomponent systems with dilute impurities, are difficult to obtain.[10] Extended x-ray absorption fine-structure spectroscopy (EXAFS) has the sensitivity to probe the structure of atoms surrounding each species of atom in the material by tuning the x-ray energy to the absorption edge of a specific element. Recently, the local structure of RE in multicomponent glasses was investigated by several researchers.[6,11–18] However, to the best of our knowledge, it is lacking information about the RE environment in low-silica calcium aluminate (LSCA) glasses. These glasses are interesting from a structural point of view, since they are formed with nontraditional network formers.[19,20] In the $CaO:Al_2O_3$ phase diagram, the region of glass formation is limited between 25 and 51 mol % of Al_2O_3.[21] The assumption for such glass formation in this binary system is the counterpolaring effect of the Ca ion on the AlO_6 complex that causes a transformation to an AlO_4 grouping,[22] which would act as a network former, such as, for example, SiO_4. However, the alkaline oxide effect on the AlO_6 group is not enough for this transformation to occur easily, so that a high cooling rate is necessary to prevent crystallization. The addition of a small amount (<10 mol %) of SiO_2, BaO, or other alkali/earth-alkali oxide allows the formation of a large amount of glass.[23–25]

Recent studies[1,26–31] of RE-doped LSCA glasses show a decrease on the hardness, glass transformation temperature, thermal diffusivity, as well as on the fluorescence quantum efficiency as the RE replaces the Al_2O_3 content. The introduction of RE in the LSCA glasses is limited to 2 mol %, beyond which crystallization occurs.[28] Er-Yb codoped LSCA glasses appeared recently as a new candidate for solid-state laser applications due to its optimized thermo-optical properties, and because it is the only oxide glass to emit fluorescence at 2.8 μm.[31] Sources of light in this wavelength are desirable for medical applications.[32] In light of its structural peculiarities, we expect that the RE environment changes as the RE content is added to the glass composition. In this work, we investigated the local environment of Er and Yb dopants and Er-Yb codopants in LSCA glasses by the EXAFS technique. The samples were prepared under vacuum conditions to prevent water contamination.

II. EXPERIMENTAL PROCEDURES

A. Sample preparation

The Er- and Yb-doped and Er-Yb-codoped LSCA glass samples were prepared from $CaCO_3$ (99%), Al_2O_3 (99.1%), MgO (97%), SiO_2 (99%), Er_2O_3 (99.99%), and Yb_2O_3 (99.99%). The glass compositions are given in Table I. The 10-g batch was melted under vacuum at 1500 °C in a graphite crucible for 2 h. The cooling was conducted moving the crucible to a cooled chamber close to room temperature, which was also under vacuum. In order to perform the EX-

TABLE I. Glass compositions (in mol %).

Sample	CaO	Al_2O_3	MgO	SiO_2	Er_2O_3	Yb_2O_3
CAGER2	58.0	27.0	6.9	8.0	0.2	
CAGER7	58.7	25.5	6.9	8.1	0.7	
CAGER15	59.8	23.1	7.0	8.2	1.5	
CAGYB2	57.8	27.2	7.0	8.0		0.2
CAGYB5	58.4	27.1	7.0	8.0		0.5
CAGYB9	58.9	25.0	7.1	8.1		0.9
CAGYB4ER4	58.6	25.5	8.1	7.1	0.4	0.4
CAGYB4ER9	59.5	23.8	7.2	8.2	0.9	0.4

AFS measurements, the samples were cut in a rectangular shape, $10\times20\times3$ mm, and polished optically.

B. EXAFS measurements

Er and Yb L_{III}-edge (8358 and 8944 eV, respectively) x-ray absorption spectra were acquired at the LNLS facility (Campinas, Brazil) on the XAS station. The LNLS storage ring is a third-generation synchrotron x-ray source, which operates at 1.37 GeV with a nominal ring current of 130 mA.[33] A Si (1 1 1) double-crystal monochromator was used. The data collection was performed in the fluorescence mode using a Si(Li) solid-state detector with energy selection (Camberra SL30165). At least three scans were collected for each sample, which were averaged to increase the quality of the experimental data. The analysis of the XAFS data was performed following the recommendations of the International Committee[34] using the WINXAS program.[35] The first step of the analysis was the extraction of the EXAFS signal, $\chi(k)$, i.e., the oscillatory part of the absorption coefficient, given by[36,37]

$$\chi(k)=\sum_j S_0^2 N_j F_j(k,\pi)\frac{\sin[2kR_j+\phi_j(k)]}{kR_j^2}e^{-2R_j/\lambda}e^{-2\sigma^2k^2},$$

where S_0^2 is the amplitude reduction factor, accounting for many-body effects, N_j is the coordination number, $F_j(k,\pi)$ is the backscattering amplitude, R_j is the nearest-neighbor distance, λ is the mean free path of the photoelectron for inelastic scattering, $2\sigma^2$ is the Debye-Waller factor, which describes the level of static and dynamic disorder, k is the wave vector of the photoelectron, and $\phi_j(k)$ is the phase shift. The $\chi(k)$ function was calculated from the absorption data, $\chi(E)=[\mu(E)-\mu_0(E)]/\mu_0(E_0)$, where the $\mu(E)$ includes absorption from the edge of interest and the EXAFS oscillations, $\mu_0(E)$ does not include EXAFS oscillations, and $\mu_0(E_0)$ is the absorption coefficient chosen systematically at a point near the edge using a single polynomial function. The E_0 value was obtained taking the second derivative inflection point of the absorption coefficient. The $\chi(E)$ signal was recalculated into k space using $k=\sqrt{2m(E-E_0)}\hbar^{-1}$ and $\mu_0(E)$ was isolated by fitting a four-rank polynomial function. Afterwards, we perform the Fourier transform (FT) of the $\chi(k)$ signal.

In order to verify the appropriateness of the use of empirical and theoretical standards to analyze the chemical environment of RE in our samples, we performed the Er edge fits in two ways. The first one was analyzing the FT of the k^2-weighted $\chi(k)$, taking into account the phase and amplitude of the standard crystalline Er_2O_3, and the second one was fitting these FT's, using the theoretical backscattering phase and amplitude functions for the various paths, calculated *ab initio* by FEFF7.[38] In this case, the ATOMS code[39] was used as a tool to generate the input files for FEFF7 using the crystallography data for Er_2O_3 and Yb_2O_3 found elsewhere.[40] The use of empirical standards means that $2\sigma^2$ is measured in a relative sense, i.e., the $2\sigma^2$ of the unknown is measured relative to the $2\sigma^2$ of the standard. With theoretical standards, the $2\sigma^2$ is measured in an absolute sense.

In the case of Yb edge fits, the analyses were carried out using only the FEFF7 phase and amplitudes. In this analysis, we obtained the RE structural parameters, coordination number CN, radial distance r, and the Debye-Waller factor $2\sigma^2$.

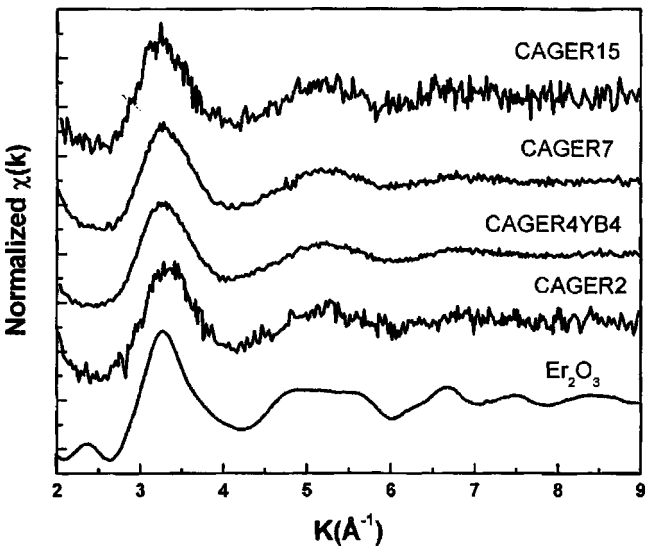

FIG. 1. Erbium L_{III}-edge EXAFS $\chi(k)$ of Er-doped low-silica calcium aluminate glasses. The reference Er_2O_3 data are also shown.

III. RESULTS

Figures 1 and 2 show Er and Yb L_{III}-edge EXAFS $\chi(k)$ data for Er- and Yb-doped LSCA glasses, as well as for the Er_2O_3 used as a model compound. The Fourier transforms of the k^2-weighted $\chi(k)$, extracted between 1.9 and 8.7 $Å^{-1}$, are showed in Figs. 3 and 4. For the crystalline Er_2O_3 we found, for the first shell, Er-O CN$=(6.0\pm0.1)$, $r=(2.24\pm0.01)$ Å, and $2\sigma^2=(0.014\pm0.002)$ $Å^2$. These results are in agreement with those reported previously by EXAFS and x-ray diffraction.[15] Fixing the CN as 6 and performing the measurement of the amplitude reduction factor from the data measured on the known standard, we obtained $S_0^2=(0.98\pm0.01)$. For those analyses performed using FEFF7, we used this S_0^2 for the Er edge fits, whereas for Yb edge fits we used $S_0^2=1$. These phase shifts are assumed to be transferable to the glass and are taken as constant in the analysis of the glass data.

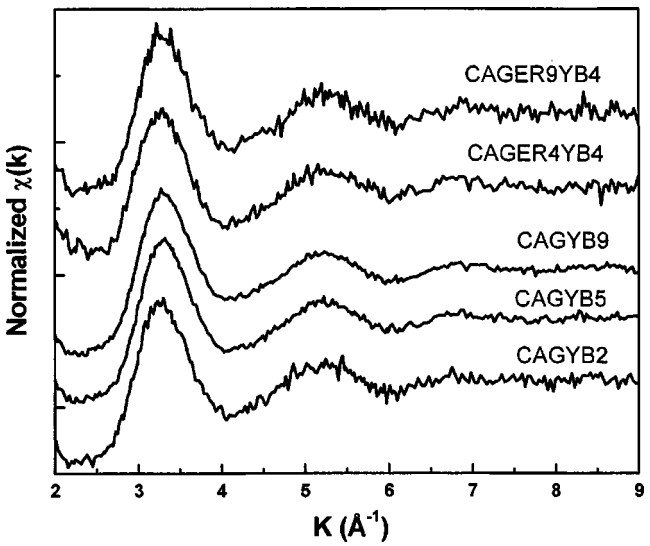

FIG. 2. Ytterbium L_{III}-edge EXAFS $\chi(k)$ of the Yb-doped low-silica calcium aluminate glasses.

Figure 5(a) shows a comparison between the fitting performed into r space using the standard Er_2O_3 phase and amplitude in relation to the FEFF7 ones for the CAGER2. In both cases, the fittings match well the experimental data. For this sample, we find, when using FEFF7, CN$=(6.5\pm0.5)$ oxygen atoms, $r=(2.24\pm0.02)$ Å, and $2\sigma^2=(0.026\pm0.004)$ Å^2, whereas using the Er_2O_3 phase and amplitudes, CN$=(6.6\pm0.5)$ oxygen atoms, $r=(2.24\pm0.01)$ Å, and $2\sigma^2=(0.013\pm0.003)$ Å^2. In the case of Er edge fits, the experimentally derived phase factors intrinsically contain a Debye-Waller component to the level of 0.014 Å^2, which is then additive with that determined for the glass, whereas the FEFF7 phases are generally derived from a $2\sigma^2=0$ model. Figure 5(b) shows the Fourier transform of the k^2-weighted $\chi(k)$ of the CAGYB5 sample, along with the theoretical fit curve obtained using the Yb_2O_3 phase and amplitude calculated by FEFF7. For this first shell, Yb-O, we find CN$=(6.2\pm0.4)$ oxygen atoms, $r=(2.19\pm0.01)$ Å, and $2\sigma^2=(0.024\pm0.006)$ Å^2.

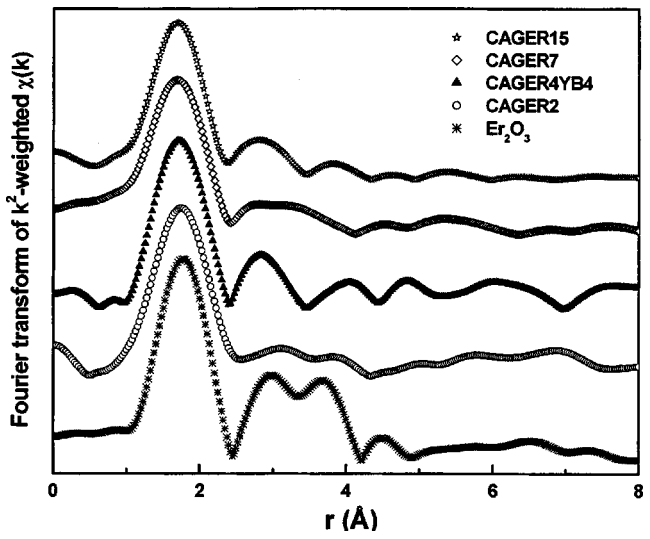

FIG. 3. Fourier transform of k^2-weighted $\chi(k)$ of the Er-doped low-silica calcium aluminate glasses data, as well as the Er_2O_3 standard.

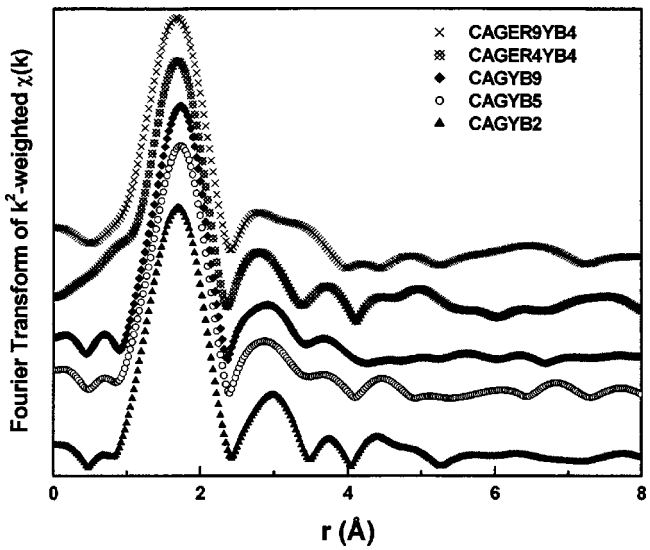

FIG. 4. Fourier transform of k^2-weighted $\chi(k)$ of the Yb-doped low-silica calcium aluminate glasses data.

The average Er and Yb coordination environments determined in the present EXAFS investigation are summarized in Table II. The measurement of uncertainties was made varying slightly the range around the FT first peak, in order to get the best-fit curve. In the case of CA glasses doped with Er^{3+}, there is a decrease of the CN from 6.5 (sample doped with 0.2 mol % Er_2O_3) to 4.7 (sample doped with 1.5 mol % Er_2O_3), a change of about 28%; the radial distance r decreases from 2.4 to 2.1 Å and $2\sigma^2$ decreases from 0.026 to 0.020 Å^2, which is within the measurements error. The CN of the Yb^{3+}-doped samples decreases from 6.4 (sample doped with 0.2 mol % of Yb_2O_3) to 5.5 atoms (sample doped with 0.9 mol % of Yb_2O_3), a change of about 15%.

For the CAGYB4ER4 sample, doped with 0.4 mol % of Er_2O_3 and codoped with 0.4 mol % of Yb_2O_3, CN$=(4.8\pm0.5)$ atoms, $r=(2.23\pm0.02)$ Å, and $2\sigma^2=(0.012\pm0.003)$ Å. The CN and $2\sigma^2$ values are smaller than those of CAGER7, which has a higher Er_2O_3 content. On the other hand, r is in the expected range. The same can be observed for the samples CAGYB4ER4 and CAGYB4ER9, when the measurements are performed in the L_{III} Yb absorption edge, where the Yb_2O_3 content is fixed at 0.4 mol %, whereas the Er_2O_3 is increased from 0.4 to 0.9 mol %. However, CN and $2\sigma^2$ varied from 5.7 to 6.2 atoms and 0.20 to 0.24 Å^2, respectively, showing a dependence on the Er_2O_3 content. For both samples, the radial distance is 2.18 Å.

Figure 6 shows the correlation map, taking into account the variation of the coordination number CN and the Debye-Waller factor $2\sigma^2$.

IV. DISCUSSION

Many works[41–50] dealing with structure arrangement in calcium aluminate glasses are concerned with the Al envi-

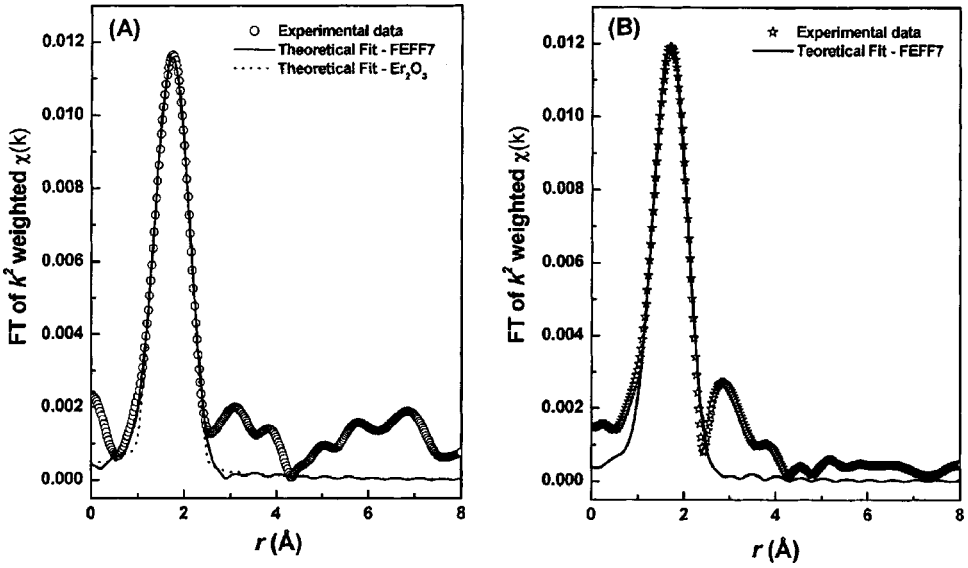

FIG. 5. In (a) is shown a comparison between the theoretical fitting for the CAGER2 sample, using the phase and amplitude of the Er_2O_3 crystalline sample, and those generated by FEFF7 software. In (b) is shown for CAGYB5 the Fourier transform along with the theoretical signal corresponding to its best-fit curve.

ronment, which appears to be tetrahedrally coordinated. It is surprising that, in spite of their optimized properties and unusual structure, there are almost no investigations about the environment of the impurities in these glasses.

Tanabe *et al.*[51] investigated the local structure of Eu^{3+}-doped calcium aluminate glasses by Mössbauer spectroscopy. The isomer shift of ^{151}Eu is around 0.9 mm/s, indicating that the CN of rare-earth ions in CA glasses is around 7 atoms. Besides, they suggested a relatively decreased Eu-O bond length and CN of Eu^{3+} in the host with a large basicity. In the case of aluminosilicate glasses, the CN was found to be between 9 and 12 atoms. In fact, our results corroborate their assumption, since we have found the CN of 6.5 atoms for those samples doped with 0.1 mol % of Er_2O_3 or Yb_2O_3. As discussed by Peters *et al.*,[11] the rare-earth environment is host-dependent, and they showed the CN ranging from 6.3 oxygen nearest-neighbor anions in the aluminosilicate glasses to 10 F in fluoride glasses. In the case of Er^{3+} TZN glasses,[13] a decrease was found in the CN as the Er_2O_3 doping increased from 0.35 up to 1.76 mol %. In this doping range, the CN decreased from 7.6 to 6.8 atoms, whereas the $2\sigma^2$ decreased from 20 to 17×10^{-3} Å^2. These variations are within the typical measurement errors of EXAFS. The CN environments of Nd and Er in phosphate glasses,[17] $(1-x)P_2O_5:xR_2O_3$ $(0.05\leqslant x\leqslant 0.25)$, exhibit a decrease of about 30%, from 8.3 to 6.3 atoms for Er-doped samples, and from 9.2 to 6.4 atoms for Nd-doped ones. In these glasses, isolated eight-coordinated RE^{3+} ions can exist for RE doping concentration $\leqslant$16.7 mol %; for greater R_2O_3 contents, isolated RE polyhedra can also exist only if the average RE CN decreases. RE clusters are expected to be present in these glasses with R_2O_3 contents >25 mol %.

Brown *et al.*[52] investigated the Yb environment in a series of Na_2O-Al_2O_3-SiO_2 glasses, and found that the Yb-O distance is 2.14 Å with a CN of ~8 for albite glass ($NaAlSi_3O_8$). In the case of depolymerized glasses ($Na_{3.3}AlSi_7O_{17}$ and $Na_2Si_3O_7$), the CN increased to ~10 atoms and r is ~2.22 Å. If 2 wt % of fluoride is added to albite glass, r increases to 2.21 Å with a CN of ~12 atoms.

TABLE II. Structural parameters (coordination number CN, bond distance r, and Debye-Waller factor $2\sigma^2$) obtained at the Er and Yb L_{III} edge of Er_2O_3 and Yb_2O_3-doped low-silica calcium aluminate glasses.

Sample	CN	r (Å)	$2\sigma^2$ (Å)
	Er-O		
CAGER2	6.5±0.5	2.24±0.02	0.026±0.004
CAGER7	5.9±0.3	2.22±0.01	0.028±0.003
CAGER15	4.7±0.3	2.21±0.01	0.020±0.003
CAGER4YB4	4.8±0.5	2.23±0.02	0.012±0.003
	Yb-O		
	CN	r (Å)	$2\sigma^2$ (Å)
CAGYB2	6.4±0.6	2.19±0.02	0.026±0.004
CAGYB5	6.2±0.4	2.19±0.01	0.024±0.006
CAGYB9	5.5±0.4	2.20±0.01	0.020±0.003
CAGER4YB4	6.2±0.5	2.18±0.02	0.024±0.003
CAGER9YB4	5.7±0.5	2.18±0.03	0.020±0.005

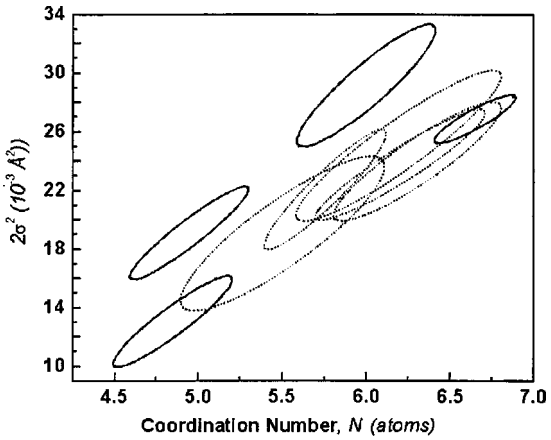

FIG. 6. Correlation map of coordination number and Debye-Waller factor for low-silica calcium aluminate glasses doped with Er^{3+} (solid curves) and Yb^{3+} (dashed curves).

Our results for LSCA show that the CN decreases from 6.5 to 4.7 atoms as the RE content increases from 0.1 up to 1.5 mol %. These results show that the Yb environment is strongly dependent on the glass composition. The radial distances Yb-O are smaller in relation to Er-O, 2.19 and 2.23 Å, respectively. This variation can be explained assuming the lanthanide contraction.[6]

It is worth noting that the CN of our Er-doped LSCA glasses, in relation to Er-doped phosphate glasses investigated by Karabulut *et al.*,[17] have a similar decrease of about 25%. But instead of a large amount of RE content, ~25 mol % added in their samples, the amount of rare earth in our LSCA glasses was ≤1.5 mol %. This suggests that the RE environment in LSCA glasses is much more susceptible to small variations in the glass composition than in phosphate glasses.

In recent works,[26–28] we showed that low amounts, ≤1.5 mol %, of RE in LSCA glasses affect slightly the thermal, optical, and mechanical properties, with variations ≤10%. For this reason we speculate that the RE content is not thoroughly responsible for this variation, since the CA glasses have a prominent tendency toward devitrification. Although in our glass compositions we had a small amount of SiO_2 and MgO to improve vitrification, we have noted, in the beginning of our studies, that the addition of small amounts of RE oxide in the glass composition enhanced the tendency to crystallization. Only after some trials did we find that the best way to obtain amorphous samples was replacing Al_2O_3 by RE oxide, which in turn led to a decrease in the Al_2O_3/CaO ratio of about 20%.

Previous structural studies[43–46] of binary CA glasses proposed that their structure consists of a continuous network of $(AlO_4)^{5-}$ tetrahedra with Ca^{2+} occupying the interstices in the network providing charge compensation for the negatively charged aluminum/oxygen tetrahedra. As the CaO is added to the composition, nonbridging oxygens (NBO's) are formed. NBO's are oxygen atoms which do not connect two tetrahedral cations or network-forming atoms, such as Si.[47] Since each oxygen acts as a bridge between two aluminum ions, the net charge on each bridged tetrahedron is −1, so that one calcium ion charge compensates two adjacent tetrahedra. McMillan *et al.*[44] suggested that the aluminum-oxygen tetrahedra become less regular as the CaO content increases, so that the tetrahedra gradually become more distorted and convert to irregular fivefold and sixfold units.

For our LSCA glasses, the Al_2O_3/CaO ratio was initially 0.463, sample CAGER2, which decreased to 0.386, sample CAGER15. It follows that, according to the above statement that extra NBO's are formed, this induces a connectivity decrease in the glass network, leading to a decrease in the glass transformation temperature (T_g).[26] Considering this fact, we can infer that the CN of our samples is affected by the Al_2O_3/CaO ratio due to the formation of NBO's, besides the RE concentration. As we plot the CN as a function of RE concentration, Fig. 7(a), and CN versus CaO/Al_2O_3 ratio, Fig. 7(b), we observe that the CN's have a similar dependence with respect to RE concentration and CaO/Al_2O_3 ratio. In both cases, the CN has a maximum value at lower RE content and lower CaO/Al_2O_3 ratio, and the opposite for the CN minimum. From a linear fit to CN versus RE content, we obtained that the gradient of the line was approximately −1/4, and for the CN versus CaO/Al_2O_3 ratio it was approximately −3/4, with a correlation factor 0.993 and 0.984, respectively.

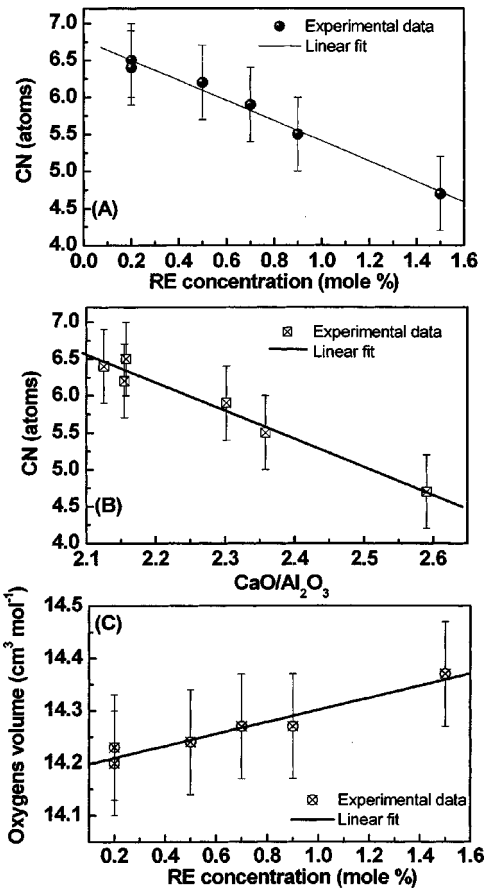

FIG. 7. (a) Coordination number as a function of rare-earth doping concentration; (b) CN as a function of the CaO/Al_2O_3 ratio; (c) oxygen volume as a function of the RE concentration.

The change in molar volume with RE substitution in aluminosilicate glasses follows the same trend of Ln_2O_3 crystals having the same coordination state.[53] Thus the structure of the aluminosilicate glasses is not significantly changed by RE substitution, except for the size of the local structure around Ln^{3+} ions; that is, the RE ions create their own sites within the glass structure.[54] According to Volf,[55] as we plot the volume of oxygen atoms versus the concentration of a given oxide, in mole percent, and the resulting curve is parallel to the ordinate *x*, all the atoms are situated in the interstices of the glass former. If this curve is ascending, it is an indication of the expansion of the glass network due to the entry of another element. In order to investigate the trend of this curve for doped RE LSCA glasses, we calculated the volume of oxygen atoms given using $V=\Sigma x_i m_i/\rho\Sigma x_i n_i$, where m_i is the molar weight of the ith oxide, ρ is the density, x_i is the molar fraction of the ith oxide, and n_i is the molar number of oxygen atoms per mole of the oxide. The results are shown in Table III and are plotted in Fig. 7(c). The resulting curve is ascending, with a correlation factor 0.967, which is an indication that the RE ions have difficulty

TABLE III. Properties of low-silica calcium aluminate glasses. ρ is the density, V_g is the glass volume, and V_O is the oxygen volume.

Sample	ρ (g/cm^3)[a]	V_g[a]	V_O
CAGER2	2.957	23.09	14.23
CAGER7	3.027	22.96	14.27
CAGER15	3.123	22.72	14.37
CAGYB2	2.960	23.08	14.20
CAGYB5	3.007	22.96	14.24
CAGYB9	3.057	22.78	14.27
CAGER4YB4	3.027	22.84	14.32
CAGER9YB4	3.099	22.72	14.35

[a]See Ref. 26.

residing on tetrahedral sites in the glass structure, and confirms their tendency to occupy octahedral sites. Hence, the bonds between the rare-earth ions and the surrounding oxygen atoms represent the weakest links in the glass structure. This assumption agrees with our previous result of a decrease of thermal and mechanical properties with an increase of RE concentration.[26]

In an earlier study[53] it was suggested that when a RE ion is placed into a rigid network of single structural units such as the SiO_4 tetrahedron, it cannot coordinate a sufficient number of NBO's and is in a higher enthalpy state, so that it forms a cluster with other ions of the same kind, in order to share the few oxygen atoms available. The difficulty for rare-earth ions to take CN's less than 8 in complex oxides is due to a large ionic radius ratio (r_{Ln}/r_0) (>0.732) and to a strong ionicity of Ln-O bonds ($\geqslant 70\%$). For this reason, the role of rare-earth ions in oxide glasses is considered as a network modifier.

Recently[28,56] it has been shown that Ca^{2+} presence in the CA glasses stiffens the glass in its resistance to compression, and the bulk modulus K is approximately twice that of SiO_2. For this reason we could speculate that there would be a formation of RE clusters in our LSCA glasses; however, the fitting of higher shells could not be obtained precisely in order to determine the formation of RE clusters. Nevertheless, in a recent work of Er-Yb codoped aluminate glasses,[31] de Souza *et al.* showed that the critical radius of interaction for $Yb^{3+} \rightarrow Er^{3+}$ is 8.37 Å, and for $Er^{3+} \rightarrow Yb^{3+}$ it is 4.71 Å, whose energy transfer for the $Yb^{3+} \rightarrow Er^{3+}$ process is 2.6 times greater than that of the $Er^{3+} \rightarrow Yb^{3+}$. Measurements of the fluorescence lifetime, τ_f, and nonradiative decay rate, τ_{NR}^{-1}, as a function of Er^{3+} concentration for similar CA glass composition[57] show that τ_f and τ_{NR}^{-1} decrease quadratically, which is attributed to the energy transfer due to electric-dipole interaction, suggesting that clusters of Er-Er are not present in these glasses.

Finally, in order to analyze statistically the variation of N and $2\sigma^2$, considering the local structure of Er^{3+} in multicomponent glasses, Peter and Walter[9] proposed the creation of a correlation map taking into account the coordination number and the Debye-Waller factor, since during the fitting we can vary both simultaneously without damage to the fit quality. Their results show that the Er^{3+} environment is host-dependent. In the case of phosphate glasses, the range of $N-2\sigma^2$ is smaller when compared to fluoride, fluorosilicate, and aluminosilicate glasses. Our results of $N-2\sigma^2$ for Er^{3+}- and Yb^{3+}-doped low-silica calcium aluminosilicate glasses show that, besides host dependence, they are also dopant-dependent. This variation is more prominent in the case of Yb^{3+}-doped glasses

V. CONCLUSIONS

Local structure environments of Er^{3+} and Yb^{3+} in low-silica calcium aluminosilicate glasses were investigated by EXAFS on the L_{III} absorption edge. The use of both empirical and theoretical standards is appropriate to analyze the RE chemical environment in doped calcium aluminate glasses. We have shown that the coordination numbers decrease about 25%, from 6.5 to 4.7 oxygen atoms around the RE ion. This decrease is attributed to an increase of NBO's due to the Al_2O_3/CaO ratio increase. For this reason, the RE ions create their own sites due to a difficulty in coordinating these NBO's.

ACKNOWLEDGMENTS

We are grateful to the LNLS staff for their valuable assistance with XAFS data collection. This work was supported under the auspices of FAPESP.

*Corresponding author. Electronic address: jsampaio@ifi.unicamp.br

[1] J. A. Sampaio, M. L. Baesso, S. Gama, A. A. Coelho, J. A. Eiras, and I. A. Santos, J. Non-Cryst. Solids **304**, 293 (2002).

[2] W. Koechner, *Solid State Laser Engineering*, 4th ed. (Springer, Berlin, 1996), pp. 28–39.

[3] *Rare Earth Doped Fiber Lasers and Amplifiers*, edited by M. J. F. Digonnet (Marcel Dekker, New York, 1993), pp. 42–50.

[4] *Laser Spectroscopy of Solids*, Topics in Applied Physics, Vol. 49, edited by W. M. Yen and P. M. Selzer (Springer-Verlag, Berlin, 1981).

[5] K. Arai, H. Namikawa, K. Kumata, T. Honda, Y. Ishii, and T. Handa, J. Appl. Phys. **59**, 3430 (1986).

[6] J. M. Cole, R. J. Newport, D. T. Bowron, R. F. Pettifer, G. Mountjoy, T. Brennan, and G. A. Saunders, J. Phys.: Condens. Matter **13**, 6659 (2001).

[7] J. A. Sampaio, T. Catunda, S. Gama, and M. L. Baesso, J. Non-Cryst. Solids **284**, 210 (2001).

[8] S. Tanabe, K. Hirao, and N. Soga, J. Am. Ceram. Soc. **75**, 503 (1992).

[9] L. Lucas, M. Chanthanasinh, M. Poulain, P. Brun, and M. J. Weber, J. Non-Cryst. Solids **27**, 273 (1978).

[10] *EXAFS Spectroscopy, Techniques and Applications*, edited by B. K. Teo and D. C. Joy (Plenum, New York, 1981), p. 163.

[11] P. M. Peters and S. N. Houde-Walter, J. Non-Cryst. Solids **239**, 162 (1998).

[12] P. M. Peters and S. N. Houde-Walter, Appl. Phys. Lett. **70**, 541 (1997).

[13] N. M. Souza Neto, A. Y. Ramos, and L. C. Barbosa, J. Non-Cryst. Solids **304**, 195 (2002).
[14] Y. Shimizugawa, N. Sawaguchi, K. Kawamura, and K. Hirao, J. Appl. Phys. **81**, 6657 (1997).
[15] M. A. Marcus and A. Polman, J. Non-Cryst. Solids **136**, 260 (1991).
[16] G. Mountjoy, J. M. Cole, T. Brennan, R. J. Newport, G. A. Saunders, and G. W. Wallidge, J. Non-Cryst. Solids **279**, 20 (2001).
[17] M. Karabulut, G. K. Marasinghe, E. Metwalli, A. K. Wittenauer, and R. K. Brow, Phys. Rev. B **65**, 104206 (2002).
[18] W. Wang, Y. Chen, and T. Hu, J. Appl. Phys. **79**, 3477 (1996).
[19] G. Y. Onoda, Jr. and S. D. Brown, J. Am. Ceram. Soc. **53**, 311 (1970).
[20] J. E. Shelby, J. Am. Ceram. Soc. **68**, 155 (1985).
[21] *Inorganic Glass-Forming Systems*, edited by H. Rawson (Academic, London, 1967), p. 317.
[22] *Glass Chemistry*, edited by W. Vogel (Springer, Berlin, 1994), p. 254.
[23] J. M. Florence, F. W. Glaze, and M. H. Black, J. Res. Natl. Bur. Stand. **55**, 231 (1955).
[24] H. C. Hafner, N. J. Kreidl, and R. A. Weidl, J. Am. Ceram. Soc. **41**, 315 (1958).
[25] J. R. Davy, Glass Technol. **19**, 33 (1978).
[26] M. L. Baesso, A. C. Bento, A. R. Duarte, A. M. Neto, L. C. M. Miranda, J. A. Sampaio, T. Catunda, S. Gama, and F. C. G. Gandra, J. Appl. Phys. **85**, 8112 (1999).
[27] J. A. Sampaio, T. Catunda, F. C. G. Gandra, S. Gama, A. C. Bento, L. C. M. Miranda, and M. L. Baesso, J. Non-Cryst. Solids **247**, 196 (1999).
[28] J. A. Sampaio, T. Catunda, A. A. Coelho, S. Gama, A. C. Bento, L. C. M. Miranda, and M. L. Baesso, J. Non-Cryst. Solids **273**, 239 (2000).
[29] E. Pecoraro, J. A. Sampaio, L. A. O. Nunes, S. Gama, and M. L. Baesso, J. Non-Cryst. Solids **277**, 73 (2000).
[30] D. F. de Sousa, J. A. Sampaio, L. A. O. Nunes, M. L. Baesso, A. C. Bento, and L. C. M. Miranda, Phys. Rev. B **62**, 3176 (2000).
[31] D. F. de Souza, L. F. C. Zonetti, M. J. V. Bell, J. A. Sampaio, L. A. O. Nunes, M. L. Baesso, A. C. Bento, and L. C. M. Miranda, Appl. Phys. Lett. **74**, 908 (1999).
[32] R. M. Dwyer and M. Bass, in *Lasers in Medicine*, edited by M. Ross (Academic, New York, 1977), Vol. 3, p. 107, and references therein.
[33] M. Abbate, F. C. Vicentin, V. Compagnon-Caihol, M. C. Rocha, and H. Toletino, J. Synchrotron Radiat. **6**, 964 (1999).
[34] F. W. Lytle, D. E. Sayers, and E. A. Stern, Physica B **158**, 701 (1989).
[35] T. Ressler, J. Phys. IV **C2**, 269 (1997).
[36] J. J. Rehr and R. C. Albers, Rev. Mod. Phys. **72**, 621 (2000).
[37] *X-ray Absorption: Principles, Applications, Techniques of EXAFS, SEXAFS and XANES*, edited by D. E. Koningsberger and R. Prins (Wiley-Interscience, New York, 1988).
[38] S. I. Zabinsky, J. J. Rehr, A. Ankudinov, R. C. Albers, and M. J. Eller, Phys. Rev. B **52**, 2995 (1995).
[39] B. Ravel, J. Synchrotron Radiat. **8**, 314 (2001).
[40] *Crystal Structures, Volume 2: Inorganic Compound* Rx_n, R_nMX_2, R_nMX_3, edited by R. W. G. Wyckoff (Wiley, New York, 1964).
[41] C. Huang and E. C. Behrman, J. Non-Cryst. Solids **128**, 310 (1991).
[42] D. A. Dutt, P. L. Higby, and D. L. Griscom, Phys. Chem. Glasses **33**, 51 (1992).
[43] G. Engelhardt, M. Nofz, K. Forkel, F. G. Wihsmann, M. Mägi, A. Samoson, and E. Lippmaa, Phys. Chem. Glasses **26**, 157 (1985).
[44] P. F. McMillan, W. T. Petuskey, B. Coté, D. Massiot, C. Landron, and J. P. Coutures, J. Non-Cryst. Solids **195**, 261 (1996).
[45] P. McMillan and B. Piriou, J. Non-Cryst. Solids **55**, 221 (1983).
[46] P. McMillan, B. Piriou, and A. Navrotsky, Geochim. Cosmochim. Acta **46**, 2021 (1982).
[47] M. Benoit, S. Ispas, and M. E. Tuckerman, Phys. Rev. B **64**, 224205 (2001).
[48] F. Fondeur and B. S. Mitchell, J. Non-Cryst. Solids **224**, 184 (1998).
[49] A. C. Hannon and J. M. Parker, J. Non-Cryst. Solids **174**, 102 (2000).
[50] B. T. Poe and P. F. McMillan, J. Am. Ceram. Soc. **77**, 1832 (1994).
[51] S. Tanabe, T. Ohyagi, T. Hanada, and N. Soga, J. Ceram. Soc. Jpn. **101**, 74 (1993).
[52] G. E. Brown, Jr., G. A. Waychunas, C. W. Ponader, W. E. Jackson, and D. A. Nckeown, J. Phys. (Paris), Colloq. **C8**, 661 (1986).
[53] S. Tanabe, K. Hirao, and N. Soga, J. Am. Ceram. Soc. **75**, 503 (1992).
[54] J. T. Kohli and J. E. Shelby, Phys. Chem. Glasses **32**, 67 (1991).
[55] M. B. Volf, *Mathematical Approach to Glass, Glass Science and Technology 9* (Elsevier, Prague, 1988).
[56] L. Hwa, K. Hsieh, and L. Liu, Mater. Chem. Phys. **78**, 105 (2002).
[57] X. Zou and T. Izumitani, J. Non-Cryst. Solids **162**, 68 (1993).